


**Beliaev damping of gapped excitations in a two-component Bose-Einstein condensate**Rukuan Wu <sup>\*</sup>*Department of Physics, Zhejiang Normal University, Jinhua 321004, China*

(Received 4 March 2024; accepted 21 May 2024; published 7 June 2024)

We investigate the Beliaev damping of gapped excitations in a homogenous two-component Bose-Einstein condensate with Rabi coupling and find different damping behavior of gapped excitations in two quantum phases. In the paramagnetic phase, due to constraints imposed by the  $\mathbb{Z}_2$  symmetry and energy-momentum conservation, the only damping channel available, that of decaying into one phonon and one new gapped mode, cannot occur unless the group velocity of the gapped modes surpasses the sound speed. Conversely, in the ferromagnetic phase, three distinct decay channels exist. Once the momentum of the excitations falls below a critical threshold, only one of these channels, that of decaying into two gapless modes, is activated, and the damping rate remains finite even at zero momentum.

DOI: [10.1103/PhysRevA.109.063314](https://doi.org/10.1103/PhysRevA.109.063314)**I. INTRODUCTION**

The elementary excitations, or quasiparticles, play a crucial role in understanding the low-energy physical properties of quantum many-body systems. When considering the residual interactions between quasiparticles, it results in the finite lifetime of excitations, which alters the fundamental properties of quantum systems, such as transport and thermalization. One well-known damping mechanism is the Beliaev-Landau damping. In the Beliaev damping, one quasiparticle decays into two new quasiparticles [1,2], while in the Landau damping, a quasiparticle absorbs thermal quasiparticles [3]. At zero temperature, the Beliaev damping is the only damping mechanism for the excitations and has been demonstrated in a wide variety of systems, including the Bose superfluids [4–14], Fermi superfluids [15], Bose-Fermi mixtures [16,17], and nonequilibrium polariton BECs [18].

Previous studies on spinor BECs mainly focus on the damping of gapless modes (phonons) [11,12], with little attention paid to gapped excitations. In contrast to discrete spectra of gapped excitations in trapped superfluids, the energy spectra of gapped excitations in uniform spinor BECs [19–22] is continuous. The Beliaev damping of the former is prohibited due to the difficulty in satisfying the energy conservation condition for discrete spectra, whereas the damping of the latter is generally feasible. The gapped excitations, including rotons in superfluid helium [23,24], optical phonons in crystals [25], and magnons in spin systems [26], have been extensively studied for their decay. Given the additional constraints on the damping channels, the decay of the gapped excitations is significantly different from that of the gapless modes [20].

In this paper, we investigate the Beliaev damping of gapped excitations in a uniform Rabi-coupled two-component

Bose-Einstein condensate (BEC) that exhibits a  $U(1) \times \mathbb{Z}_2$  symmetry. The condensate's ground state can manifest as an unpolarized paramagnetic phase, wherein the densities of both components ( $n_1$  and  $n_2$ ) are equal, or as a partially polarized ferromagnetic phase, with unequal component densities [19,27]. The system exhibits two branches of excitations: gapless and gapped modes [19,28]. Interactions among excitations of the same or different branches give rise to a greater diversity of damping channels in spinor BECs compared to their single-component counterparts. Nevertheless, when we narrow our focus to low-momentum excitations, this diversity is significantly diminished. As shown in previous research [12], gapless modes with low momentum possess such minimal energy that they decay into just two phonons, maintaining the familiar  $q^5$  scaling with momenta. Although low-momentum gapped excitations, owing to their higher energy, might intuitively suggest the presence of multiple damping channels, our research surprisingly shows that this is not the case. In this paper, we first derive a general formula for the damping rate using Fermi's golden rule. Our analysis reveals the existence of three potential decay channels for the gapped modes. Specifically, a gapped quasiparticle can decay into two gapless quasiparticles or, alternatively, into a pair of new gapped quasiparticles, or even into a gapless quasiparticle and a fresh gapped quasiparticle. However, subsequent investigations highlight that the  $\mathbb{Z}_2$  symmetry, along with the energy-momentum conservation condition, imposes significant constraints on these damping channels. In the paramagnetic phase, the  $\mathbb{Z}_2$  symmetry prohibits the first two decay channels, while the third, though permissible, is stringently governed by the energy-momentum conservation condition. This latter channel only manifests when the group velocity of the gapped excitations surpasses the speed of sound. Conversely, in the ferromagnetic phase, where  $\mathbb{Z}_2$  symmetry is broken, the damping rate of low-momentum gapped excitations is predominantly influenced by the first channel, owing to the prevailing constraints imposed by energy-momentum conservation.

<sup>\*</sup>Contact author: [arkuan@zjnu.cn](mailto:arkuan@zjnu.cn)

The remainder of this paper is structured as follows. In Sec. II, we employ the perturbation method to derive the generalized Beliaev damping rate applicable to two-component Bose-Einstein condensates. Subsequently, in Secs. III and IV, we delve into the specific damping rates of gapped excitations in the paramagnetic and ferromagnetic phases, respectively. Lastly, Sec. V provides a comprehensive summary of our findings.

## II. GENERAL EXPRESSION FOR THE BELIAEV DAMPING RATE

We consider a homogenous two-component BEC, in which the two components interact through pure contact and Rabi coupling interactions. The relevant Hamiltonian is written in the form [12]

$$\hat{H} = \int d^3\mathbf{r} \sum_{j=1,2} \left[ \frac{\hbar^2}{2m} |\nabla \hat{\psi}_j(\mathbf{r})|^2 + \frac{\hbar\Omega}{2} \hat{\psi}_j^\dagger(\mathbf{r}) \hat{\psi}_{\bar{j}}(\mathbf{r}) \right] + \int d^3\mathbf{r} \sum_{i,j=1,2} \frac{g_{ij}}{2} \hat{\psi}_i^\dagger(\mathbf{r}) \hat{\psi}_j^\dagger(\mathbf{r}) \hat{\psi}_j(\mathbf{r}) \hat{\psi}_i(\mathbf{r}), \quad (1)$$

where  $j, \bar{j} = 1, 2$ , and  $j \neq \bar{j}$ .  $\hat{\psi}_1(\mathbf{r})$  and  $\hat{\psi}_2(\mathbf{r})$  are the annihilation field operators for the two-component bosonic atoms. The coupling constants,  $g_{11}$ ,  $g_{22}$ , and  $g_{12}$  denote the intraspecies and interspecies interactions, respectively. For simplicity, we assume  $g_{11} = g_{22} = g$  for the intraspecies coupling constants. Additionally, we introduce the Rabi frequency  $\Omega$  to describe the coherent coupling between the two components, assuming  $\Omega > 0$  throughout this paper. The system has a  $U(1) \times \mathbb{Z}_2$  symmetry, where  $U(1)$  corresponds to the total atom number being conserved, and  $\mathbb{Z}_2$  corresponds to the exchange of the two components. The total condensate density is  $n_0$ . In the case of  $(g - g_{12})n_0 + \hbar\Omega > 0$ , the ground state exhibits a paramagnetic phase characterized by  $n_1 = n_2 = n_0/2$ , where  $n_1$  and  $n_2$  represent the condensate density of the two components. This phase preserves the  $\mathbb{Z}_2$  symmetry. On the other hand, when  $(g - g_{12})n_0 + \hbar\Omega < 0$ , the ground state is a doubly degenerate ferromagnetic phase with  $(n_1 - n_2)_\pm = \pm n_0 \sqrt{1 - \eta^2}$ , where  $\eta = \hbar\Omega / (g - g_{12})n_0$  [19]. In this phase, the  $\mathbb{Z}_2$  symmetry is broken [12]. The phase transition between these two phases has been realized by the experiment [29].

The atomic field can be expanded in the plane-wave basis  $\hat{\psi}_j(\mathbf{r}) = \frac{1}{\sqrt{V}} \sum e^{i\mathbf{q}\cdot\mathbf{r}/\hbar} \hat{a}_{j,\mathbf{q}}$ . In the weak-coupling regime, the lowest moment state ( $q = 0$ ) is macroscopically occupied, and  $\hat{a}_{j,0}, \hat{a}_{j,0}^\dagger \approx (-1)^{j+1} \sqrt{N_j}$ . Here  $N_j$  is the atomic number of the component, and the total number of atoms is given by  $N = N_1 + N_2$ . As  $N_j$  is much larger than the occupation of all other single-particle modes, the Hamiltonian can be rearranged based on the order of the ladder operators ( $\hat{a}_{i,\mathbf{q}}$  and  $\hat{a}_{i,\mathbf{q}}^\dagger$ , with  $\mathbf{q} \neq 0$ ). By neglecting the smallest fourth-order term containing only single-particle operators, the Hamiltonian can be approximately expressed as  $\hat{H} \approx \hat{H}_0 + \hat{H}_2 + \hat{H}_3$ . The zeroth-order term  $\hat{H}_0$  is a constant value and can be dropped. The second-order term  $\hat{H}_2$  is a Bogoliubov-type

quadratic Hamiltonian, and one obtains

$$\hat{H}_2 = \sum_{j,\mathbf{q}} \left[ h_j \hat{a}_{j,\mathbf{q}}^\dagger \hat{a}_{j,\mathbf{q}} + \frac{g}{2} n_j (\hat{a}_{j,\mathbf{q}}^\dagger \hat{a}_{j,-\mathbf{q}}^\dagger + \hat{a}_{j,\mathbf{q}} \hat{a}_{j,-\mathbf{q}}) \right] + \sum_{\mathbf{q}} \left( \frac{\hbar\Omega}{2} \hat{a}_{1,\mathbf{q}}^\dagger \hat{a}_{2,\mathbf{q}} - g_{12} \sqrt{n_1 n_2} \hat{a}_{1,\mathbf{q}}^\dagger \hat{a}_{2,\mathbf{q}} - g_{12} \sqrt{n_1 n_2} \hat{a}_{1,\mathbf{q}}^\dagger \hat{a}_{2,-\mathbf{q}} + \text{H.c.} \right), \quad (2)$$

where  $h_j = \frac{q^2}{2m} + \frac{g}{2}(3n_j - n_j) + \frac{g_{12}}{2}(n_j - n_j) + \frac{\hbar\Omega n_0}{4\sqrt{n_1 n_2}}$ . The third-order term  $\hat{H}_3$  describes the scattering process of excitations and is given by

$$\hat{H}_3 = \frac{1}{\sqrt{V}} \sum_{j,\mathbf{p},\mathbf{q}} (-1)^{j+1} \sqrt{n_j} (g \hat{a}_{j,\mathbf{p}}^\dagger \hat{a}_{j,\mathbf{q}-\mathbf{p}}^\dagger \hat{a}_{j,\mathbf{q}} + g_{12} \hat{a}_{j,\mathbf{p}}^\dagger \hat{a}_{j,\mathbf{q}-\mathbf{p}}^\dagger \hat{a}_{\bar{j},\mathbf{q}} + \text{H.c.}). \quad (3)$$

By introducing the quasiparticle operators  $\hat{b}_{\sigma,\mathbf{q}}$  and  $\hat{b}_{\sigma,\mathbf{q}}^\dagger$  which satisfy the Bogoliubov transformations

$$\hat{a}_{i,\mathbf{q}} = \sum_{\sigma=\alpha,\beta} (u_{i,1,\mathbf{q}}^\sigma \hat{b}_{\sigma,\mathbf{q}} + u_{i,2,-\mathbf{q}}^\sigma \hat{b}_{\sigma,-\mathbf{q}}^\dagger), \quad (4)$$

the second-order term  $\hat{H}_2$  can be rewritten in the diagonal form as  $\hat{H}_2 = \sum_{\sigma,\mathbf{q}} \epsilon_{\mathbf{q}}^\sigma \hat{b}_{\sigma,\mathbf{q}}^\dagger \hat{b}_{\sigma,\mathbf{q}} + \text{constant}$ , where  $\alpha$  and  $\beta$  denote the gapless mode and the gapped mode, respectively. The functions  $u$  are the solutions of the Bogoliubov-de Gennes (BdG) equations [19]

$$h_j u_{j,k,\mathbf{q}}^\sigma + g n_j u_{j,\bar{k},\mathbf{q}}^\sigma + \left( \frac{\hbar\Omega}{2} - g_{12} \sqrt{n_1 n_2} \right) u_{j,k,\mathbf{q}}^\sigma - g_{12} \sqrt{n_1 n_2} u_{j,\bar{k},-\mathbf{q}}^\sigma = (-1)^{k+1} \epsilon_{\mathbf{q}}^\sigma u_{j,k,\mathbf{q}}^\sigma. \quad (5)$$

The third-order term  $\hat{H}_3$  can also be rewritten using the quasiparticle operators, resulting in the expression

$$\hat{H}_3 = \frac{1}{2\sqrt{V}} \sum_{\sigma,\sigma',\tilde{\sigma}} \sum_{\mathbf{p},\mathbf{q}} (B_{\mathbf{p},\mathbf{q}-\mathbf{p},\mathbf{q}}^{\sigma\sigma'\tilde{\sigma}} \hat{b}_{\sigma,\mathbf{p}}^\dagger \hat{b}_{\sigma',\mathbf{q}-\mathbf{p}}^\dagger \hat{b}_{\tilde{\sigma},\mathbf{q}} + \text{H.c.}). \quad (6)$$

We have ignored terms such as  $\hat{b}\hat{b}\hat{b}$  or  $\hat{b}^\dagger\hat{b}^\dagger\hat{b}^\dagger$  as they do not conserve the energy and will not contribute to the decay process. The first term of Eq. (6) describes the Beliaev decay process, where one  $\tilde{\sigma}$  mode decays into one  $\sigma$  mode and another  $\sigma'$  mode. The scattering matrix element  $B_{\mathbf{p},\mathbf{p}'}^{\sigma\sigma'\tilde{\sigma}}$  is given by

$$B_{\mathbf{p},\mathbf{p}'}^{\sigma\sigma'\tilde{\sigma}} = \sum_{j,k=1,2} \{ (-1)^{j+1} \sqrt{n_j} [ 2g (u_{j,k,\mathbf{p}}^\sigma u_{j,k,\mathbf{p}'}^{\sigma'} + u_{j,k,\mathbf{p}}^{\sigma'} u_{j,k,\mathbf{p}}^\sigma + u_{j,k,\mathbf{p}}^\sigma u_{j,k,\mathbf{p}'}^{\sigma'} + u_{j,k,\mathbf{p}}^{\sigma'} u_{j,k,\mathbf{p}}^\sigma) + g_{j\bar{j}} (u_{j,k,\mathbf{p}}^\sigma u_{j,\bar{k},\mathbf{p}'}^{\sigma'} + u_{j,k,\mathbf{p}}^{\sigma'} u_{j,\bar{k},\mathbf{p}}^\sigma) ] + (-1)^{\bar{j}+1} \sqrt{n_{\bar{j}}} g_{j\bar{j}} (u_{j,k,\mathbf{p}}^\sigma u_{j,k,\mathbf{p}'}^{\sigma'} + u_{j,k,\mathbf{p}}^{\sigma'} u_{j,k,\mathbf{p}}^\sigma + u_{j,k,\mathbf{p}}^\sigma u_{j,\bar{k},\mathbf{p}'}^{\sigma'} + u_{j,k,\mathbf{p}}^{\sigma'} u_{j,\bar{k},\mathbf{p}}^\sigma) \} u_{j,k,\mathbf{q}}^{\tilde{\sigma}}. \quad (7)$$

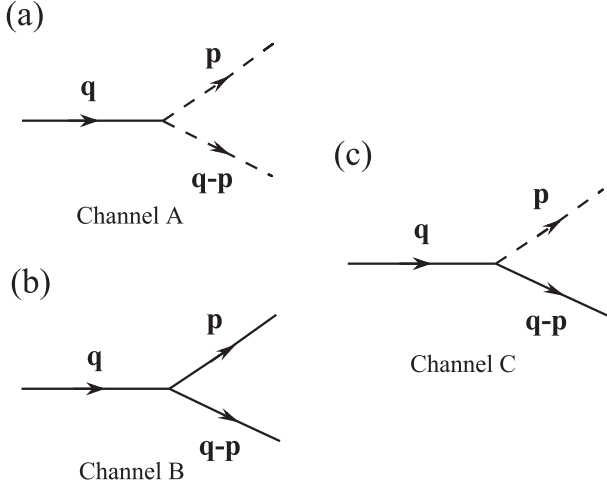


FIG. 1. Schematic representations of three decay channels for a gapped mode (solid line) with the momentum  $\mathbf{q}$ . (a) Channel A depicts decay into two gapless modes (dashed lines). (b) Channel B illustrates decay into two new gapped modes. (c) Channel C shows decay into one gapless mode and one new gapped mode.

According to Fermi's golden rule, the Beliaev damping rate of the  $\tilde{\sigma}$  mode at zero temperature can be written as

$$\begin{aligned} \gamma_{\tilde{\sigma}}^{\tilde{\sigma}} &= \frac{\pi}{2V} \sum_{\sigma, \sigma', \mathbf{p}} |B_{\mathbf{p}, \mathbf{q}-\mathbf{p}, \mathbf{q}}^{\sigma \sigma' \tilde{\sigma}}|^2 \delta(\epsilon_{\tilde{\sigma}}^{\tilde{\sigma}} - \epsilon_{\mathbf{p}}^{\sigma} - \epsilon_{\mathbf{q}-\mathbf{p}}^{\sigma'}) \\ &= \frac{1}{16\pi^2 \hbar^3} \int \sum_{\sigma, \sigma'} |B_{\mathbf{p}, \mathbf{q}-\mathbf{p}, \mathbf{q}}^{\sigma \sigma' \tilde{\sigma}}|^2 \delta(\epsilon_{\tilde{\sigma}}^{\tilde{\sigma}} - \epsilon_{\mathbf{p}}^{\sigma} - \epsilon_{\mathbf{q}-\mathbf{p}}^{\sigma'}) d\mathbf{p}, \end{aligned} \quad (8)$$

which coincides with our previous result obtained by the time-dependent mean-field approach (see Supplemental Material of Ref. [11]). The Beliaev decay of the gapless mode ( $\alpha$  mode) has been previously examined [12], revealing that the damping rate  $\gamma_{\tilde{\sigma}}^{\alpha}$  is proportional to  $q^5$  in the paramagnetic phase [12]. In this paper, we focus on the Beliaev decay of the gapped excitation ( $\beta$  mode). Referring to Eq. (8), we identify three distinct decay channels for the gapped mode: channel A, which involves a decay into two gapless modes [illustrated in Fig. 1(a)]; channel B, where the decay results in two new gapped modes [depicted in Fig. 1(b)]; and channel C, which entails a decay into one gapless mode and one new gapped mode [shown in Fig. 1(c)]. It should be noted that  $B_{\mathbf{p}, \mathbf{p}', \mathbf{q}}^{\alpha \beta \beta}$  and  $B_{\mathbf{p}', \mathbf{p}, \mathbf{q}}^{\beta \alpha \beta}$  describe the same decay process.

### III. DAMPING IN THE PARAMAGNETIC PHASE

In the paramagnetic phase,  $n_1 = n_2 = n_0/2$ , which preserves the  $\mathbb{Z}_2$  symmetry. This symmetry significantly simplifies the expressions for the Bogoliubov spectrums and amplitudes, which can be derived by solving Eqs. (5). The energy spectrums of the gapless and gapped modes are given by  $\epsilon_{\mathbf{q}}^{\alpha} = \sqrt{\epsilon_{\mathbf{q}}[\epsilon_{\mathbf{q}} + (g + g_{12})n_0]}$  and  $\epsilon_{\mathbf{q}}^{\beta} = \sqrt{(\epsilon_{\mathbf{q}} + \hbar\Omega)[\epsilon_{\mathbf{q}} + \hbar\Omega + (g - g_{12})n_0]}$ , respectively, where  $\epsilon_{\mathbf{q}} = q^2/2m$ . The gapless mode represents the density wave, while

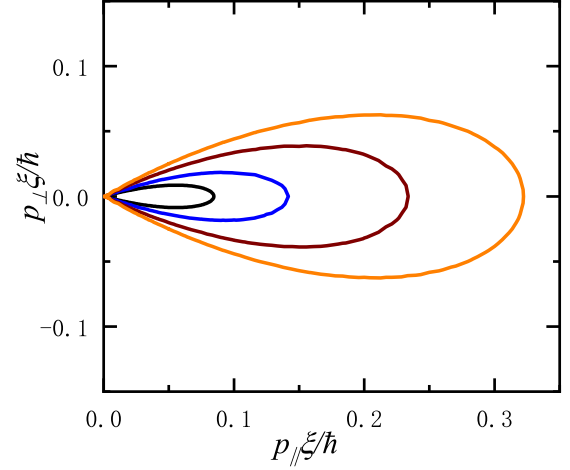


FIG. 2. Momentum manifolds allowed by the momentum-energy conservation in the  $p_{\parallel} - p_{\perp}$  plane for various momenta  $\mathbf{q}$  under  $g_{12}/g = 1.5$  and  $\hbar\Omega/gn_0 = 0.6$ . Here, the  $p_{\parallel}$  and  $p_{\perp}$  represent the components parallel and perpendicular to  $\mathbf{q}$ , respectively. The momentum is expressed in units of  $\hbar/\xi$ , where the coherent length  $\xi = \hbar/\sqrt{mgn_0}$ . The manifolds correspond to  $q\xi/\hbar = 1.12$  (innermost), 1.15, 1.20, and 1.25 (outermost). Notably, the threshold momentum  $q_c = 1.08\hbar/\xi$ , below which the manifold disappears.

the gapped mode characterizes the spin wave [19]. The Bogoliubov amplitudes  $u$  can be written as

$$\begin{aligned} u_{1,k,\mathbf{q}}^{\alpha} &= -u_{2,k,\mathbf{q}}^{\alpha} = \frac{1}{2\sqrt{2}} \left[ \sqrt{\frac{\epsilon_{\mathbf{q}}}{\epsilon_{\mathbf{q}}^{\alpha}}} - (-1)^k \sqrt{\frac{\epsilon_{\mathbf{q}}^{\alpha}}{\epsilon_{\mathbf{q}}}} \right], \quad (9) \\ u_{1,k,\mathbf{q}}^{\beta} &= u_{2,k,\mathbf{q}}^{\beta} = \frac{1}{2\sqrt{2}} \left( \sqrt{\frac{\epsilon_{\mathbf{q}} + \hbar\Omega}{\epsilon_{\mathbf{q}}^{\beta}}} - (-1)^k \sqrt{\frac{\epsilon_{\mathbf{q}}^{\beta}}{\epsilon_{\mathbf{q}} + \hbar\Omega}} \right). \end{aligned} \quad (10)$$

Substitute the condition  $u_{j,k,\mathbf{q}}^{\alpha} = -u_{j,k,\mathbf{q}}^{\alpha}$  and  $u_{j,k,\mathbf{q}}^{\beta} = u_{j,k,\mathbf{q}}^{\beta}$  into Eq. (7), then it is straightforward to verify that  $B_{\mathbf{p}, \mathbf{q}-\mathbf{p}, \mathbf{q}}^{\alpha \alpha \beta} = B_{\mathbf{p}, \mathbf{q}-\mathbf{p}, \mathbf{q}}^{\beta \beta \beta} = 0$ . Consequently, only channel C, which involves the decay into one gapless mode and one new gapped excitation, is activated. Since  $B_{\mathbf{p}, \mathbf{q}-\mathbf{p}, \mathbf{q}}^{\alpha \beta \beta} = B_{\mathbf{q}-\mathbf{p}, \mathbf{p}, \mathbf{q}}^{\beta \alpha \beta}$ , the Beliaev damping rate given by Eq. (8) can be simplified to

$$\gamma_{\mathbf{q}} = \frac{1}{8\pi^2 \hbar^3} \int |B_{\mathbf{p}, \mathbf{q}-\mathbf{p}, \mathbf{q}}^{\alpha \beta \beta}|^2 \delta(\epsilon_{\mathbf{q}}^{\beta} - \epsilon_{\mathbf{p}}^{\alpha} - \epsilon_{\mathbf{q}-\mathbf{p}}^{\beta}) d\mathbf{p}. \quad (11)$$

The momentum-energy conservation condition  $\epsilon_{\mathbf{q}}^{\beta} = \epsilon_{\mathbf{p}}^{\alpha} + \epsilon_{\mathbf{q}-\mathbf{p}}^{\beta}$  is not always satisfied for this decay channel. For example, as shown in Fig. 2, under the conditions  $g_{12}/g = 1.5$  and  $\hbar\Omega/gn_0 = 0.6$ , the conservation condition is violated once the momentum  $q$  of the gapped mode falls below  $1.08\hbar/\xi$ . Defining the group velocities of the quasiparticles as  $c_{\mathbf{q}}^{\sigma} = \partial\epsilon_{\mathbf{q}}^{\sigma}/\partial q$ , it can be concluded that the energy conservation condition holds only when  $c_{\mathbf{q}}^{\beta} \geq c_0^{\alpha}$ , where the sound speed  $c_0^{\alpha} = \sqrt{(g + g_{12})n_0/2m}$ . The threshold momentum  $q_c$  is determined by the condition  $c_{q_c}^{\beta} = c_0^{\alpha}$ , and damping becomes activated when  $q \geq q_c$ . This damping process resembles the Cherenkov effect, in which radiation is emitted by a charged

particle moving through a material at a speed exceeding the velocity of the light in the medium.

Now let us consider the situation where  $q$  is slightly larger than  $q_c$ , that is,  $0 < (q - q_c)\xi/\hbar \ll 1$ , where the coherent length  $\xi = \hbar/\sqrt{mg n_0}$ . As shown in Fig. 2, if  $0 < (q - q_c)\xi/\hbar \ll 1$ , the permissible momentum  $p\xi/\hbar \ll 1$ . Therefore, the momentum-energy conservation condition can be approximately written as  $|\nabla_{\mathbf{q}}\epsilon_{\mathbf{q}}^\beta| * p \cos \theta \approx c_0^\alpha p$ , where  $\theta$  is the angle between  $\mathbf{q}$  and  $\mathbf{p}$ . Since  $|\nabla_{\mathbf{q}}\epsilon_{\mathbf{q}}^\beta| \approx c_{q_c}^\beta = c_0^\alpha$ , it can be obtained that  $\cos \theta \approx 1$ . This implies that when  $0 < q - q_c \ll 1$ ,  $\mathbf{p}$  and  $\mathbf{q}$  are nearly in the same direction (see Fig. 2). Therefore, the  $\delta$  function can be approximately written as

$$\delta(\epsilon_{\mathbf{q}}^\beta - \epsilon_{\mathbf{p}}^\alpha - \epsilon_{\mathbf{q}-\mathbf{p}}^\beta) \approx \frac{1}{c_0^\alpha p} \delta(\cos \theta - 1). \quad (12)$$

The integral range of  $p$  in Eq. (11) can be determined by solving the energy-momentum conservation condition  $\epsilon_{\mathbf{q}}^\beta = \epsilon_{\mathbf{p}}^\alpha + \epsilon_{\mathbf{q}-\mathbf{p}}^\beta$ . By addressing the conservation equation under the assumption that  $\mathbf{p}$  and  $\mathbf{q}$  are aligned in the same direction, it can be derived that the lower integral limit of  $\mathbf{p}$  is 0, and the upper integral limit is  $2(q - q_c)$ .

Moreover, for  $0 < q - q_c \ll 1$ , the matrix element can be approximately expressed as

$$B_{\mathbf{p}, \mathbf{q}-\mathbf{p}, \mathbf{q}}^{\alpha\beta\beta} \approx \frac{A_{q_c} \sqrt{p}}{2\sqrt{\sqrt{2mn_0}(g + g_{12})^{\frac{3}{2}}}}, \quad (13)$$

where

$$A_{q_c} = \left[ 4g - \frac{(g - g_{12})^2 n_0}{\frac{q_c^2}{2m} + \hbar\Omega + (g - g_{12})n_0} \right] \sqrt{\frac{q_c^2}{2m}}. \quad (14)$$

Notably, we have replaced  $\cos \theta$  with 1 in Eq. (13) to simplify the formula. Utilizing these approximations and through straightforward calculations, we find that the Beliaev damping rate of the gapped excitation in the paramagnetic phase can be written as

$$\gamma_{\mathbf{q}} = \frac{A_{q_c}^2 (q - q_c)^3}{6\pi \hbar^3 (g + g_{12})^2 n_0} \Theta(q - q_c), \quad (15)$$

where  $\Theta(x)$  is the step function. When  $q < q_c$  ( $v_q^\beta < c_0^\alpha$ ),  $\gamma_{\mathbf{q}} = 0$  and the gapped excitations will not decay. And when  $q \geq q_c$  ( $v_q^\beta \geq c_0^\alpha$ ), at the leading order,  $\gamma_{\mathbf{q}}$  increases rapidly as  $(q - q_c)^3$ . The results of the damping rate in the paramagnetic phase are presented in Fig. 3. With a fixed ratio of  $g_{12}/g = 1.5$ , it is evident that even as  $\hbar\Omega/g n_0$  approaches the ferromagnetic transition point, the threshold behavior of  $\gamma_{\mathbf{q}}$  still persists. Consequently, Eq. (15) remains valid in the vicinity of the transition point. Furthermore, if  $\hbar\Omega \gg |(g_{12} - g)n_0|$ ,  $q_c \approx \sqrt{(g + g_{12})mn_0/2} = mc_0^\alpha$ , and the damping rate can be simplified as

$$\gamma_{\mathbf{q}} \approx \frac{2g^2 (q - q_c)^3}{3\pi \hbar^3 (g + g_{12})} \Theta(q - q_c), \quad (16)$$

which is independent of the Rabi frequency  $\Omega$  (see Fig. 3).

#### IV. DAMPING IN THE FERROMAGNETIC PHASE

Without loss of generality, we assume the ground state with  $n_j = n_0[1 - (-1)^j \sqrt{1 - \eta^2}]/2$  for the ferromagnetic phase.

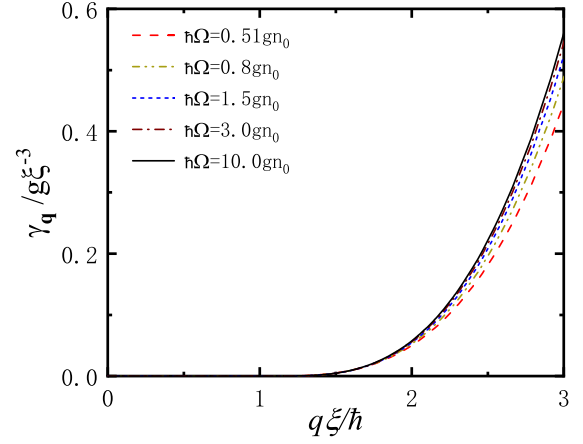


FIG. 3. The Beliaev damping rate  $\gamma_{\mathbf{q}}$  of gapped excitations in the paramagnetic phase, fixing  $g_{12}/g = 1.5$ . We take  $\hbar\Omega/g n_0 = 0.51, 0.8, 1.5, 3.0, \text{ and } 10.0$ , and the corresponding threshold momenta  $q_c = 1.066 \hbar/\xi, 1.091 \hbar/\xi, 1.108 \hbar/\xi, 1.115 \hbar/\xi, \text{ and } 1.118 \hbar/\xi$ . Experimentally, based on the data in Ref. [28], we can set the parameters  $g n_0/\hbar = 3000$  Hz,  $\xi = 1 \mu\text{m}$ , and  $g\xi^{-3}/\hbar = 30$  Hz.

The corresponding solutions of BdG equations (5) have been derived by Tommasini *et al.* [30], and only the main results are reviewed in this paper. We introduce three new dressed coupling constants  $\Lambda_{1n_0} = [g(n_1^2 + n_2^2) + 2g_{12}n_1n_2]$ ,  $\Lambda_{2n_0} = 2(g - g_{12})n_1n_2$ , and  $\Lambda_{12n_0} = (g - g_{12})\sqrt{n_1n_2}(n_2 - n_1)$ . Additionally, we define two effective kinetic energies:  $\varepsilon_{1,\mathbf{q}} = \frac{q^2}{2m}$  and  $\varepsilon_{2,\mathbf{q}} = \frac{q^2}{2m} + \frac{\hbar\Omega n_0}{2\sqrt{n_1n_2}}$ . Hence, the Bogoliubov spectrums can be written as follows [30]:

$$\epsilon_{\mathbf{q}}^\sigma = \left\{ \frac{1}{2}(\omega_{1,\mathbf{q}}^2 + \omega_{2,\mathbf{q}}^2) \pm \frac{1}{2}[(\omega_{1,\mathbf{q}}^2 - \omega_{2,\mathbf{q}}^2)^2 + 16\Lambda_{12}^2 \varepsilon_{1,\mathbf{q}} \varepsilon_{2,\mathbf{q}}]^{1/2} \right\}^{1/2}, \quad (17)$$

where the minus sign and the plus sign correspond to gapless and gapped modes, respectively, and  $\omega_{j,\mathbf{q}} = \sqrt{\varepsilon_{j,\mathbf{q}}^2 + 2\Lambda_{j,\mathbf{q}}\varepsilon_{j,\mathbf{q}}}$ . To simplify the formulas of the Bogoliubov eigenvectors, we define

$$\sin \varphi_{\mathbf{q}} = \frac{1}{\sqrt{2}} \left( 1 - \frac{\omega_{1,\mathbf{q}}^2 - \omega_{2,\mathbf{q}}^2}{\epsilon_{\mathbf{q}}^{\beta 2} - \epsilon_{\mathbf{q}}^{\alpha 2}} \right)^{1/2},$$

$$\cos \varphi_{\mathbf{q}} = \frac{1}{\sqrt{2}} \left( 1 + \frac{\omega_{1,\mathbf{q}}^2 - \omega_{2,\mathbf{q}}^2}{\epsilon_{\mathbf{q}}^{\beta 2} - \epsilon_{\mathbf{q}}^{\alpha 2}} \right)^{1/2},$$

$\Gamma_{j,\sigma,\mathbf{q}} = \sqrt{\varepsilon_{j,\mathbf{q}}/\epsilon_{\mathbf{q}}^\sigma}$ ,  $\sin \vartheta = \sqrt{n_1/n_0}$ , and  $\cos \vartheta = \sqrt{n_2/n_0}$ . As a result, the components of the eigenvectors corresponding to the gapless and gapped modes can be written as follows [30]:

$$u_{1,k,\mathbf{q}}^\alpha = \frac{\Gamma_{1,\alpha,\mathbf{q}}^2 - (-1)^k}{2\Gamma_{1,\alpha,\mathbf{q}}} \sin \varphi_{\mathbf{q}} \sin \vartheta$$

$$+ \frac{\Gamma_{2,\alpha,\mathbf{q}}^2 - (-1)^k}{2\Gamma_{2,\alpha,\mathbf{q}}} \cos \varphi_{\mathbf{q}} \cos \vartheta, \quad (18)$$

$$u_{2,k,\mathbf{q}}^\alpha = -\frac{\Gamma_{1,\alpha,\mathbf{q}}^2 - (-1)^k}{2\Gamma_{1,\alpha,\mathbf{q}}} \sin \varphi_{\mathbf{q}} \cos \vartheta$$

$$+ \frac{\Gamma_{2,\alpha,\mathbf{q}}^2 - (-1)^k}{2\Gamma_{2,\alpha,\mathbf{q}}} \cos \varphi_{\mathbf{q}} \sin \vartheta, \quad (19)$$

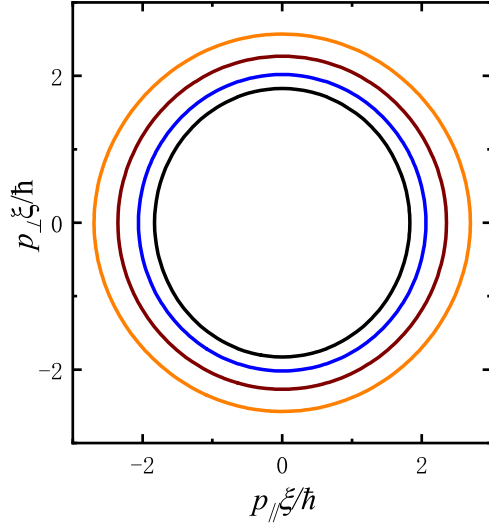


FIG. 4. Momentum manifolds allowed by the energy-momentum conservation in the  $p_{\parallel} - p_{\perp}$  plane for various momenta  $\mathbf{q}$  in the ferromagnetic phase. We take  $g_{12}/g = 10.0$  and  $\hbar\Omega/gn_0 = 7.0$ . The manifolds correspond to  $q\xi/\hbar = 0.1$  (innermost), 1.5, 2.5, and 3.5 (outermost).

$$u_{1,k,\mathbf{q}}^{\beta} = \frac{\Gamma_{2,\beta,\mathbf{q}}^2 - (-1)^k}{2\Gamma_{2,\beta,\mathbf{q}}} \sin \varphi_{\mathbf{q}} \cos \vartheta - \frac{\Gamma_{1,\beta,\mathbf{q}}^2 - (-1)^k}{2\Gamma_{1,\beta,\mathbf{q}}} \cos \varphi_{\mathbf{q}} \sin \vartheta, \quad (20)$$

$$u_{2,k,\mathbf{q}}^{\beta} = \frac{\Gamma_{2,\beta,\mathbf{q}}^2 - (-1)^k}{2\Gamma_{2,\beta,\mathbf{q}}} \sin \varphi_{\mathbf{q}} \sin \vartheta + \frac{\Gamma_{1,\beta,\mathbf{q}}^2 - (-1)^k}{2\Gamma_{1,\beta,\mathbf{q}}} \cos \varphi_{\mathbf{q}} \cos \vartheta. \quad (21)$$

It can be proved that the matrix elements  $B_{\mathbf{p},\mathbf{q}-\mathbf{p},\mathbf{q}}^{\sigma\sigma'\beta}$  of all three decay processes are nonzero in the ferromagnetic phase. Nevertheless, due to the constraint of the energy-momentum conservation, channels B and C are not activated if the momentum  $q$  is below the critical values. We introduce two threshold momenta  $q_{c1}$  and  $q_{c2}$  which satisfy the conditions  $\epsilon_{\mathbf{q}_{c1}}^{\beta} = 2\epsilon_{\mathbf{q}_{c1}/2}^{\beta}$  and  $c_{q_{c2}}^{\beta} = c_0^{\alpha}$ , respectively. Channels B and C become active only when  $q \geq q_{c1}$  and  $q \geq q_{c2}$ , respectively. It can be proved that  $q_{c1} > q_{c2}$ . Consequently, for  $q < q_c = q_{c2}$ , only channel A, which corresponds to the decay into two gapless modes, contributes to the damping rate. In such a situation, the Beliaev damping rate of the gapped excitation can be simplified to

$$\gamma_{\mathbf{q}} = \frac{1}{16\pi^2\hbar^3} \int |B_{\frac{\mathbf{q}}{2}+\mathbf{p},\frac{\mathbf{q}}{2}-\mathbf{p},\mathbf{q}}^{\alpha\alpha\beta}|^2 \delta(\epsilon_{\mathbf{q}}^{\beta} - \epsilon_{\frac{\mathbf{q}}{2}+\mathbf{p}}^{\alpha} - \epsilon_{\frac{\mathbf{q}}{2}-\mathbf{p}}^{\alpha}) d\mathbf{p}. \quad (22)$$

As shown in Fig. 4, when  $q$  approaches 0, the curve satisfying the energy-momentum conservation smoothly transitions into a circle with a radius  $p_0$ . This implies that, for the gapped modes with low momentum, only the gapless modes with the momentum close to  $p = p_0$  contribute to the decay. For  $q \ll 1$ , the excitation energies can be approximately

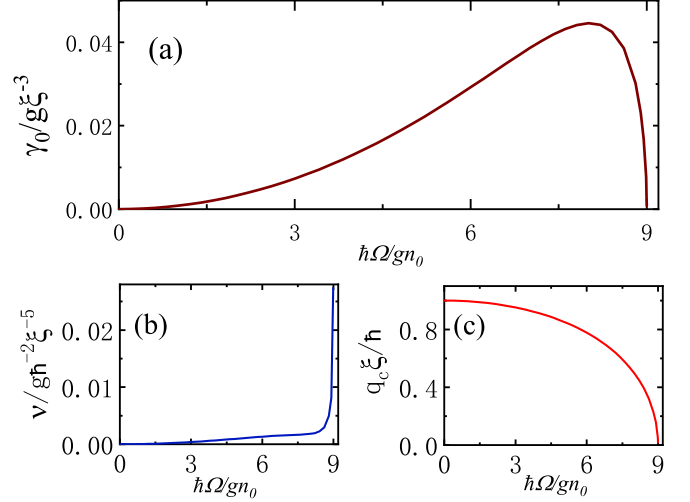


FIG. 5. (a) The Beliaev damping rate for zero momentum  $\gamma_0$  as the function of  $\Omega$ . (b) The parameter  $\nu$  as the function of  $\Omega$ . (c) The critical momentum  $q_c$  as the function of  $\Omega$ . In all plots, we take  $g_{12}/g = 10.0$ . Experimentally, we can set  $gn_0/h = 3000$  Hz,  $\xi = 1$   $\mu\text{m}$ , and  $g\xi^{-3} = 30$  Hz.

written as  $\epsilon_{\mathbf{p}}^{\alpha} \approx \epsilon_{p_0}^{\alpha} + c_{p_0}^{\alpha}(p - p_0) + \frac{1}{2}w_{p_0}^{\alpha}(p - p_0)^2$  and  $\epsilon_{\mathbf{q}}^{\beta} \approx \epsilon_0^{\beta} + \frac{1}{2}w_0^{\beta}q^2$ , where  $w_q^{\sigma} = \partial^2\epsilon_{\mathbf{q}}^{\sigma}/\partial q^2$ . Moreover, in this low-momentum regime, the matrix element can be approximated to the second order of  $q$  and is given by

$$B_{\frac{\mathbf{q}}{2}+\mathbf{p},\frac{\mathbf{q}}{2}-\mathbf{p},\mathbf{q}}^{\alpha\alpha\beta} \approx \lambda_1 + (\lambda_2 + \lambda_3 \cos^2 \theta)q^2, \quad (23)$$

where we replace the integration variable  $p$  with  $\cos \theta$  using the energy-momentum conservation condition. The details of the calculations and the expression of  $\lambda_j$  can be found in the Appendix. By the straightforward calculation for Eq. (22), we obtain the Beliaev damping rate of the gapped excitations in the ferromagnetic phase

$$\gamma_{\mathbf{q}} = \gamma_0 + \nu q^2 \quad \text{for } q < q_c, \quad (24)$$

where the damping rate for zero momentum  $\gamma_0 = \lambda_1^2 p_0^2 / 8\pi \hbar^3 c_{p_0}^{\alpha}$ , and the coefficient of the second-order term is given by

$$\nu = \frac{\lambda_1^2 p_0 (w_{p_0}^{\alpha} - 6w_0^{\beta}) (p_0 w_{p_0}^{\alpha} - 2c_{p_0}^{\alpha})}{192\pi \hbar^3 c_{p_0}^{\alpha 3}} + \frac{8p_0^2 \lambda_1 (3\lambda_2 + \lambda_3) - \lambda_1^2}{96\pi \hbar^3 c_{p_0}^{\alpha}}.$$

Equation (24) remains valid for  $q < q_c$ . In this regime, channel A is the sole active channel. In contrast to the paramagnetic phase, where the damping exhibits a threshold behavior, the ferromagnetic phase displays a consistently nonzero damping rate for gapped excitations. Specifically, the gapped mode with zero momentum decays at the rate  $\gamma_0$ , producing a pair of gapless modes with momenta  $\mathbf{p}_0$  and  $-\mathbf{p}_0$ . The difference between  $\gamma_{\mathbf{q}}$  and  $\gamma_0$ , denoted as  $\gamma_{\mathbf{q}} - \gamma_0$ , experiences a rapid increase proportional to  $q^2$ . The functional dependencies of  $\gamma_0$ ,  $\nu$ , and  $q_c$  with respect to the Rabi frequency  $\Omega$  are clearly depicted in Fig. 5. Notably, as  $\Omega$  approaches 0, the scattering matrix element gradually vanishes,

leading to a corresponding decrease in the damping rate, with  $\gamma_{\mathbf{q}}$  ultimately approaching 0.

At the critical transition point, characterized by  $(g - g_{12})n_0 + \hbar\Omega = 0$ , the gap in  $\beta$  mode vanishes, resulting in a linear spectrum at low momenta. Consequently, our approximate method for estimating the damping rate becomes inapplicable at this phase transition point. Notably, at this phase transition point, the  $\alpha$  and  $\beta$  modes of the ferromagnetic phase degenerate into the  $\beta$  and  $\alpha$  modes of the paramagnetic phase, respectively. As emphasized in Ref. [12], at the critical point, channel A continues to dominate the damping behavior, and the damping rate  $\gamma_{\mathbf{q}}$  is proportional to the momentum  $q$ . Consequently, the  $\beta$  mode of the ferromagnetic phase is not well-defined at the transition point.

## V. SUMMARY

In summary, our investigation focuses on the Beliaev damping of gapped excitations in a coherently coupled two-component Bose-Einstein condensate (BEC). Our findings reveal strikingly different damping behaviors across two quantum phases. In the paramagnetic phase, the damping process is constrained by the  $\mathbb{Z}_2$  symmetry and energy-momentum conservation, resulting in a threshold behavior characterized by  $\gamma_{\mathbf{q}} \propto (q - q_c)^3$ . Notably, gapped excitations decay exclusively into one phonon and one new gapped mode, a process that becomes active only when the group velocity of the excitations exceeds the sound speed—an analogy to the Cherenkov effect observed in electromagnetic fields. By contrast, in the ferromagnetic phase, gapped modes always decay into two gapless modes for momenta below a critical value, exhibiting a damping rate characterized by  $\gamma_{\mathbf{q}} - \gamma_0 \propto q^2$ . Unlike the threshold behavior of damping gapless modes in quasi-two-dimensional dipolar BECs [13], our findings in this paper do not have additional constraints on system dimension, potentially simplifying experimental implementation. Our theoretical predictions can be experimentally validated by measuring the damping rates of the gapped modes or utilizing Bragg spectroscopy techniques referenced in Refs. [7–9].

## ACKNOWLEDGMENTS

The authors would like to thank K. Gao, Z. Liang, and C. Gao for their insightful discussions. This work is financially supported by the National Natural Science Foundation of China under Grant No. 11975208.

## APPENDIX: GENERAL FORMULAS FOR THE FERROMAGNETIC PHASE

As discussed before, in the ferromagnetic phase, only channel A contributes to the damping rate for  $q < \min(q_{c1}, q_{c2})$ , and the Beliaev damping rate of the gapped

excitations can be simplified to

$$\gamma_{\mathbf{q}} = \frac{1}{16\pi^2\hbar^3} \int |B_{\frac{\mathbf{q}}{2}+\mathbf{p}, \frac{\mathbf{q}}{2}-\mathbf{p}, \mathbf{q}}^{\alpha\alpha\beta}|^2 \delta(\epsilon_{\mathbf{q}}^{\beta} - \epsilon_{\frac{\mathbf{q}}{2}+\mathbf{p}}^{\alpha} - \epsilon_{\frac{\mathbf{q}}{2}-\mathbf{p}}^{\alpha}) d\mathbf{p}. \quad (\text{A1})$$

For clarity, we define  $\mathcal{F}_{j,k,q}^{\alpha} = \partial u_{j,k,q}^{\alpha} / \partial q$  and  $\mathcal{G}_{j,k,q}^{\alpha} = \partial^2 u_{j,k,q}^{\alpha} / \partial q^2$ . When  $q \ll 1$ , one can use the following expansions for the functions  $u_{j,k,\mathbf{p}}^{\sigma}$ :

$$u_{j,k, \frac{\mathbf{q}}{2} \pm \mathbf{p}}^{\alpha} \approx u_{j,k, \mathbf{p}_0}^{\alpha} + \mathcal{F}_{j,k, p_0}^{\alpha} \left( \left| \frac{\mathbf{q}}{2} \pm \mathbf{p} \right| - p_0 \right) + \frac{1}{2} \mathcal{G}_{j,k, p_0}^{\alpha} \left( \left| \frac{\mathbf{q}}{2} \pm \mathbf{p} \right| - p_0 \right)^2, \quad (\text{A2})$$

$$u_{j,j,\mathbf{q}}^{\beta} \approx \frac{1}{2} \mathcal{G}_{j,j,0}^{\beta} q^2, \quad (\text{A3})$$

$$u_{j,\bar{j},\mathbf{q}}^{\beta} \approx u_{j,\bar{j},0}^{\beta} + \frac{1}{2} \mathcal{G}_{j,\bar{j},0}^{\beta} q^2. \quad (\text{A4})$$

The excitation energies can be approximated as  $\epsilon_{\mathbf{p}}^{\alpha} \approx \epsilon_{\mathbf{p}_0}^{\alpha} + c_{p_0}^{\alpha} (p - p_0) + \frac{1}{2} w_{p_0}^{\alpha} (p - p_0)^2$  and  $\epsilon_{\mathbf{q}}^{\beta} \approx \epsilon_0^{\beta} + \frac{1}{2} w_0^{\beta} q^2$ , where  $w_q^{\sigma} = \partial^2 \epsilon_{\mathbf{q}}^{\sigma} / \partial q^2$ . Consequently, the condition of the energy-momentum conservation can be approximately expressed as

$$\frac{1}{2} w_0^{\beta} q^2 \approx c_{p_0}^{\alpha} \left( \left| \frac{\mathbf{q}}{2} + \mathbf{p} \right| - p_0 \right) + c_{p_0}^{\alpha} \left( \left| \frac{\mathbf{q}}{2} - \mathbf{p} \right| - p_0 \right) + \frac{1}{2} w_{p_0}^{\alpha} \left( \left| \frac{\mathbf{q}}{2} + \mathbf{p} \right| - p_0 \right)^2 + \frac{1}{2} w_{p_0}^{\alpha} \left( \left| \frac{\mathbf{q}}{2} - \mathbf{p} \right| - p_0 \right)^2. \quad (\text{A5})$$

With the help of the approximate expression

$$\left| \frac{\mathbf{q}}{2} \pm \mathbf{p} \right| \approx p + \frac{q}{2} \cos \theta + \frac{q^2 \sin^2 \theta}{8p_0},$$

one can derive the relationship between  $p$  and  $\theta$  that fulfills the energy-momentum conservation:

$$p \approx \tilde{p} = p_0 + \left( \frac{w_0^{\beta}}{4c_{p_0}^{\alpha}} - \frac{w_{p_0}^{\alpha} \cos^2 \theta}{8c_{p_0}^{\alpha}} - \frac{\sin^2 \theta}{8p_0} \right) q^2. \quad (\text{A6})$$

Therefore, this leads to the conclusion that

$$\delta(\epsilon_{\mathbf{q}}^{\beta} - \epsilon_{\frac{\mathbf{q}}{2}+\mathbf{p}}^{\alpha} - \epsilon_{\frac{\mathbf{q}}{2}-\mathbf{p}}^{\alpha}) \approx \left( \frac{1}{2c_{p_0}^{\alpha}} + \frac{q^2 \cos^2 \theta (p_0^2 w_{p_0}^{\alpha 2} - c_{p_0}^{\alpha 2})}{16p_0^2 c_{p_0}^{\alpha 3}} + \frac{q^2 (c_{p_0}^{\alpha 2} - 2p_0^2 w_{p_0}^{\alpha} w_0^{\beta})}{16p_0^2 c_{p_0}^{\alpha 3}} \right) \delta(p - \tilde{p}). \quad (\text{A7})$$

Substitute Eqs. (A2), (A3), (A4), and (A6) into Eq. (7), and then the matrix element can be approximately written as

$$B_{\frac{\mathbf{q}}{2}+\mathbf{p}, \frac{\mathbf{q}}{2}-\mathbf{p}, \mathbf{q}}^{\alpha\alpha\beta} \approx \lambda_1 + (\lambda_2 + \lambda_3 \cos^2 \theta) q^2, \quad (\text{A8})$$

where

$$\lambda_1 = \sum_{j=1,2} (-1)^{j+1} 2\sqrt{n_j} \{ g u_{j,\bar{j},\mathbf{p}_0}^{\alpha} u_{j,\bar{j},0}^{\beta} (2u_{j,j,\mathbf{p}_0}^{\alpha} + u_{j,\bar{j},\mathbf{p}_0}^{\alpha}) + g_{12} u_{j,j,\mathbf{p}_0}^{\alpha} [(u_{j,j,\mathbf{p}_0}^{\alpha} + u_{j,\bar{j},\mathbf{p}_0}^{\alpha}) u_{j,j,0}^{\beta} + u_{j,\bar{j},\mathbf{p}_0}^{\alpha} u_{j,\bar{j},0}^{\beta}] \},$$

$$\begin{aligned}
\lambda_2 = & \sum_{j,k=1,2} (-1)^{j+1} \sqrt{n_j} \{ g u_{j,k,\mathbf{p}_0}^\alpha (u_{j,k,\mathbf{p}_0}^\alpha + 2u_{j,\bar{k},\mathbf{p}_0}^\alpha) \mathcal{G}_{j,k,0}^\beta + g_{12} u_{j,k,\mathbf{p}_0}^\alpha [u_{j,\bar{k},\mathbf{p}_0}^\alpha \mathcal{G}_{j,k,0}^\beta + (u_{j,k,\mathbf{p}_0}^\alpha + u_{j,\bar{k},\mathbf{p}_0}^\alpha) \mathcal{G}_{j,k,0}^\beta] \} \\
& + \frac{w_0^\beta}{2v_{p_0}^\alpha} \sum_{j=1,2} (-1)^{j+1} \sqrt{n_j} \{ 2g u_{j,\bar{j},0}^\beta [u_{j,\bar{j},\mathbf{p}_0}^\alpha \mathcal{F}_{j,j,p_0}^\alpha + (u_{j,j,\mathbf{p}_0}^\alpha + u_{j,\bar{j},\mathbf{p}_0}^\alpha) \mathcal{F}_{j,\bar{j},p_0}^\alpha] + g_{12} u_{j,j,0}^\beta [u_{j,j,\mathbf{p}_0}^\alpha \mathcal{F}_{j,j,p_0}^\alpha \\
& + u_{j,\bar{j},\mathbf{p}_0}^\alpha \mathcal{F}_{j,\bar{j},p_0}^\alpha + (u_{j,j,\mathbf{p}_0}^\alpha + u_{j,\bar{j},\mathbf{p}_0}^\alpha) \mathcal{F}_{j,\bar{j},p_0}^\alpha] + g_{12} u_{j,\bar{j},0}^\beta [u_{j,\bar{j},\mathbf{p}_0}^\alpha \mathcal{F}_{j,\bar{j},p_0}^\alpha + u_{j,j,\mathbf{p}_0}^\alpha \mathcal{F}_{j,j,p_0}^\alpha] \}, \\
\lambda_3 = & \frac{1}{4} \sum_{j=1,2} (-1)^{j+1} \sqrt{n_j} \{ 2g u_{j,\bar{j},0}^\beta [(u_{j,j,\mathbf{p}_0}^\alpha + u_{j,\bar{j},\mathbf{p}_0}^\alpha) \mathcal{G}_{j,\bar{j},p_0}^\alpha + u_{j,\bar{j},\mathbf{p}_0}^\alpha \mathcal{G}_{j,j,p_0}^\alpha - (\mathcal{F}_{j,\bar{j},p_0}^\alpha + 2\mathcal{F}_{j,j,p_0}^\alpha) \mathcal{F}_{j,\bar{j},p_0}^\alpha] \\
& + g_{12} u_{j,\bar{j},0}^\beta (u_{j,j,\mathbf{p}_0}^\alpha \mathcal{G}_{j,\bar{j},p_0}^\alpha + u_{j,\bar{j},\mathbf{p}_0}^\alpha \mathcal{G}_{j,j,p_0}^\alpha - 2\mathcal{F}_{j,\bar{j},p_0}^\alpha \mathcal{F}_{j,\bar{j},p_0}^\alpha) + g_{12} u_{j,j,0}^\beta [(u_{j,j,\mathbf{p}_0}^\alpha + u_{j,\bar{j},\mathbf{p}_0}^\alpha) \mathcal{G}_{j,j,p_0}^\alpha \\
& + u_{j,\bar{j},\mathbf{p}_0}^\alpha (\mathcal{G}_{j,j,p_0}^\alpha + \mathcal{G}_{j,\bar{j},p_0}^\alpha) - 2\mathcal{F}_{j,j,p_0}^\alpha (\mathcal{F}_{j,j,p_0}^\alpha + \mathcal{F}_{j,\bar{j},p_0}^\alpha)] \} \\
& - \frac{w_{p_0}^\alpha}{4v_{p_0}^\alpha} \sum_{j=1,2} (-1)^{j+1} \sqrt{n_j} \{ 2g u_{j,\bar{j},0}^\beta [u_{j,\bar{j},\mathbf{p}_0}^\alpha \mathcal{F}_{j,j,p_0}^\alpha + (u_{j,j,\mathbf{p}_0}^\alpha + u_{j,\bar{j},\mathbf{p}_0}^\alpha) \mathcal{F}_{j,\bar{j},p_0}^\alpha] + g_{12} u_{j,\bar{j},0}^\beta (\mathcal{F}_{j,j,p_0}^\alpha u_{j,\bar{j},\mathbf{p}_0}^\alpha \\
& + \mathcal{F}_{j,\bar{j},p_0}^\alpha u_{j,j,\mathbf{p}_0}^\alpha) + g_{12} u_{j,j,0}^\beta [u_{j,j,\mathbf{p}_0}^\alpha (\mathcal{F}_{j,j,p_0}^\alpha + \mathcal{F}_{j,\bar{j},p_0}^\alpha) + (u_{j,j,\mathbf{p}_0}^\alpha + u_{j,\bar{j},\mathbf{p}_0}^\alpha) \mathcal{F}_{j,j,p_0}^\alpha] \}.
\end{aligned}$$

- 
- [1] S. T. Beliaev, ZhETF **34**, 417 (1958) [*Sov. Phys. JETP* **7**, 289 (1958)].
- [2] S. T. Beliaev, ZhETF **34**, 433 (1958) [*Sov. Phys. JETP* **7**, 299 (1958)].
- [3] L. Pitaevskii and S. Stringari, *Phys. Lett. A* **235**, 398 (1997).
- [4] W. V. Liu, *Phys. Rev. Lett.* **79**, 4056 (1997).
- [5] S. Giorgini, *Phys. Rev. A* **57**, 2949 (1998).
- [6] E. Hodby, O. M. Maragò, G. Hechenblaikner, and C. J. Foot, *Phys. Rev. Lett.* **86**, 2196 (2001).
- [7] N. Katz, J. Steinhauer, R. Ozeri, and N. Davidson, *Phys. Rev. Lett.* **89**, 220401 (2002).
- [8] D. S. Jin, J. R. Ensher, M. R. Matthews, C. E. Wieman, and E. A. Cornell, *Phys. Rev. Lett.* **77**, 420 (1996).
- [9] M.-O. Mewes, M. R. Andrews, N. J. van Druten, D. M. Kurn, D. S. Durfee, C. G. Townsend, and W. Ketterle, *Phys. Rev. Lett.* **77**, 988 (1996).
- [10] J. Zhang, C. Eigen, W. Zheng, J. A. P. Glidden, T. A. Hilker, S. J. Garratt, R. Lopes, N. R. Cooper, Z. Hadzibabic, and N. Navon, *Phys. Rev. Lett.* **126**, 060402 (2021).
- [11] R. Wu and Z. Liang, *Phys. Rev. Lett.* **121**, 180401 (2018).
- [12] A. Recati and F. Piazza, *Phys. Rev. B* **99**, 064505 (2019).
- [13] S. S. Natu and S. Das Sarma, *Phys. Rev. A* **88**, 031604(R) (2013).
- [14] R. M. Wilson and S. Natu, *Phys. Rev. A* **93**, 053606 (2016).
- [15] G. Bighin, L. Salasnich, P. A. Marchetti, and F. Toigo, *Phys. Rev. A* **92**, 023638 (2015).
- [16] W. Zheng and H. Zhai, *Phys. Rev. Lett.* **113**, 265304 (2014).
- [17] J. H. Pixley, X. Li, and S. Das Sarma, *Phys. Rev. Lett.* **114**, 225303 (2015).
- [18] M. Van Regemortel, W. Casteels, I. Carusotto, and M. Wouters, *Phys. Rev. A* **96**, 053854 (2017).
- [19] M. Abad and A. Recati, *Eur. Phys. J. D* **67**, 148 (2013).
- [20] Y. Kawaguchi and M. Ueda, *Phys. Rep.* **520**, 253 (2012).
- [21] T.-L. Ho and S. Zhang, *Phys. Rev. Lett.* **107**, 150403 (2011).
- [22] Y. Li, G. I. Martone, L. P. Pitaevskii, and S. Stringari, *Phys. Rev. Lett.* **110**, 235302 (2013).
- [23] K. Bedell, D. Pines, and A. Zawadowski, *Phys. Rev. B* **29**, 102 (1984).
- [24] K. H. Andersen, J. Bossy, J. C. Cook, O. G. Randl, and J.-L. Ragazzoni, *Phys. Rev. Lett.* **77**, 4043 (1996).
- [25] P. G. Klemens, *Phys. Rev.* **148**, 845 (1966).
- [26] A. Kolezhuk and S. Sachdev, *Phys. Rev. Lett.* **96**, 087203 (2006).
- [27] R. Cominotti, A. Berti, C. Dulin, C. Rogora, G. Lamporesi, I. Carusotto, A. Recati, A. Zenesini, and G. Ferrari, *Phys. Rev. X* **13**, 021037 (2023).
- [28] R. Cominotti, A. Berti, A. Farolfi, A. Zenesini, G. Lamporesi, I. Carusotto, A. Recati, and G. Ferrari, *Phys. Rev. Lett.* **128**, 210401 (2022).
- [29] T. Zibold, E. Nicklas, C. Gross, and M. K. Oberthaler, *Phys. Rev. Lett.* **105**, 204101 (2010).
- [30] P. Tommasini, E. J. V. de Passos, A. F. R. de Toledo Piza, M. S. Hussein, and E. Timmermans, *Phys. Rev. A* **67**, 023606 (2003).